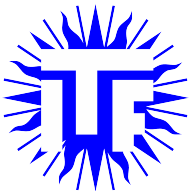

Universiteit Utrecht

MASTER THESIS

Theoretical description of the bulk movement of kinesin motors

Author:
Christophoros Eseroglou (Anemopoulos)

Supervisors:
Dr. Florian Berger
Dr. Joost de Graaf
Dr. Rene van Roij

June 30, 2021

Ἔν πάσι γὰρ τοὶς φυσικοὶς ἐνεστὶ τὶ θαυμαστὸν
"Everywhere in nature there is something admirable."

ΑΡΙΣΤΟΤΕΛΗΣ

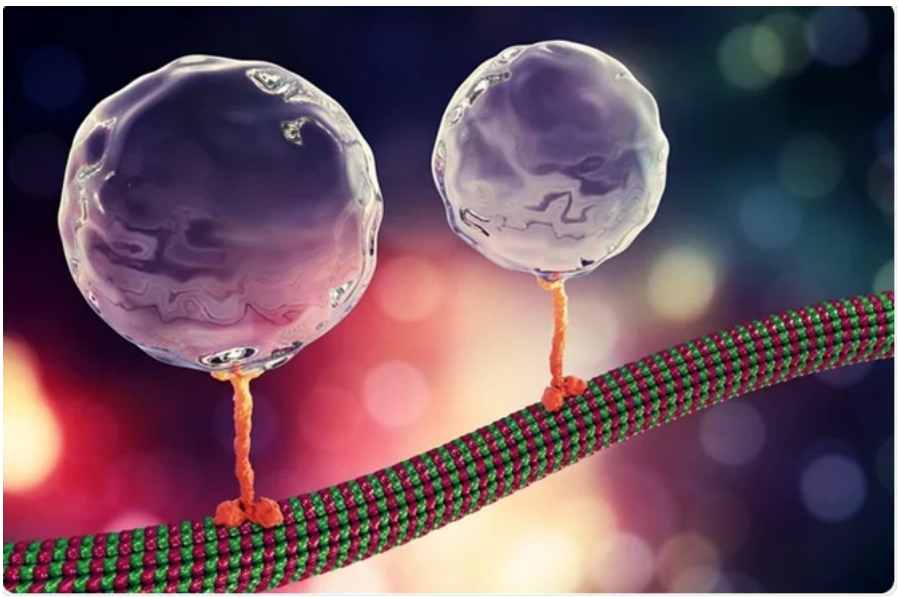

Intracellular transport: kinesin motor-proteins transport cargo vesicles along microtubule filaments. (3D illustration by Kon and Shutterstock)

Abstract

During growth, a nerve cell creates protrusions that are called neurites. The intracellular active transport of the proteins is based on kinesin molecules walking on microtubules that have a chiral symmetry and thus a direction. The direction of this movement is towards the +END of the microtubule. Estimates suggest that in neurites 80% of microtubules are aligned in such a way that kinesin molecules walk to the tip of the neurite. In sharp contrast, recent experiments found that kinesin molecules move collectively toward the cell body, away from the tip of the neurite. So far, there is no explanation on this unexpected observation. In this thesis, we introduce a mathematical description of the collective kinesin movement and investigate three different possible underlying mechanisms for the observed reversal. The most possible mechanism assumes that through cell signaling kinesin molecules exclusively can bind to different subsets of microtubules pointing either toward or away from the cell body. For this model, we approximate the full mathematical system of transport-reaction equations with an equation for biased diffusion and fit the parameters so we reproduce the experimental data and describe quantitatively the environment changes that the cell induces.

Contents

Chapter 1

Introduction

The function of the nervous system relies on a complex architecture of neuronal networks. The basic units of these networks are neurons, which are highly polarized cells with unique shapes and functions. How neurons grow into their specific shape and acquire their function is not well understood. The growth of neurons can be studied in neuronal cell culture. The main stages of neuron growth in culture are depicted in figure 1.1.

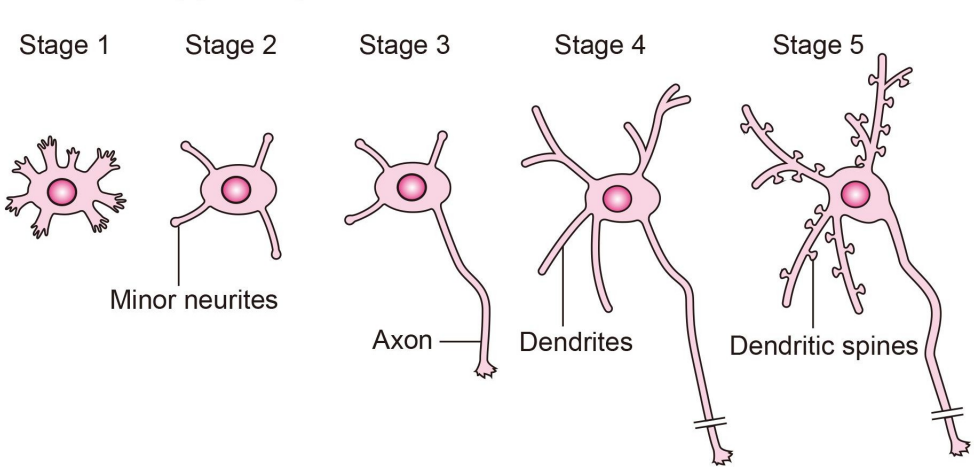

Figure 1.1: *Growth stages of neurons, reproduced from [7]. Stage 1-2: A neuron after mitosis, growing its neurites. Stage 2-3: One neurite is becoming the future axon. Stage 4-5: Stage 4-5: After development, one neurites became the axon and the other neurites became dendrites with spines.*

During their growth, neurons create protrusions, which are called neurites. One of them becomes the axon, whereas the others become dendrites. The proteins needed for this development are synthesized in the cell body. Consequently, proteins need to be transported

to the end of the growing neurites. Since neurons are usually long, passive transport via diffusion is not sufficiently quick, as the following back-of-the-envelope calculation shows. The diffusion coefficient for particles of size 100 in the cytosol is

$$D = 1\ \mu m^2/s.$$

Therefore for a typical axon of length 1 mm transport of these particles via diffusion would require

$$t = \frac{1\ mm^2}{2D} = 500\ s$$

or approximately 8.5 minutes. For comparison typical reaction in cells such as protein synthesis have a characteristic time in order of seconds. For that reason, active transport of proteins is necessary to efficiently transport material to the distal end. Newly synthesized proteins are carried by molecular motors, which walk on microtubules by converting chemical-free energy from ATP hydrolysis into mechanical work. The structure of microtubules is chiral, allowing us to define a plus and a minus end. Molecular motors bind and unbind to these microtubules. When they are bound they walk to a specific end of the microtubule. Kinesin molecules, which are a specific type of molecular motors and are of our interest, move to the plus end. In neurites, approximately 80% of microtubules have their plus end to the tip of the neurite. How the material is unloaded at specific locations and how motors are subsequently recycled is an active field of research [13]. However, the most accepted view of this process is that motors move to the developing parts, where the bounded proteins are released and used. Then motors unbind and either diffuse back to the neurite or are degraded into smaller parts. This procedure then should result in a directed movement of kinesins towards the end of the neurite. However, recent experimental results indicate, that in stages 1 and 2 of neural growth a large amount of kinesin molecules is transferred back to the cell body and then to another neurite. In this thesis, we introduce a systematic and quantitative description of possible mechanisms that connect the single molecule dynamics to the bulk movement as observed in experiments. For the remainder of the thesis, we refer to this process as “backward movement” because kinesin molecules move backward to the cell body. This thesis aims to provide a first insight into the physical mechanism of this phenomenon and what might cause it.

To answer this question, we examine three hypotheses. The first and the second hypothesis build on the idea that the cell creates an environment in the axon where either the diffusion coefficient or the binding rate respectively depend on space and time. The main idea of the third hypothesis is that the cell forces the kinesin molecules to bind to the minority of the microtubules that are aligned with their +END at the cell body and therefore kinesin molecules move back, while at the same time a remodeling of the physical properties of the environment prevents unbound kinesin molecules to diffuse away into the cytosol. Such a remodeling of the complex environment within cells could be attributed to induced

polymerization or depolymerization of actin filaments which form networks to provide mechanical support of a cell. Interestingly, induced polymerization of actin results in a wave pattern that has a similar speed as the bulk movement of the kinesin molecules [6].

This thesis is structured as follows: In chapter 2, we introduce the main biological concepts and physical phenomena underlying our theoretical descriptions. Then, in chapters 3-5, we examine the hypotheses and present the corresponding results. Finally, in chapter 6 we conclude that the explanation that agrees the most with the experiment is the third hypothesis. We suggest further experiments that will allow us to obtain better insights into this process, which should focus on changing the environmental conditions of the experiment to indirectly change the speed and number of the kinesin motors.

Chapter 2

Background

In this chapter, we present the main physical and biological concepts that we formalize into theoretical descriptions.

2.1 Experimental evidence

In figures 2.1, 2.2 we present experimental images that show the movement of kinesin molecules in neurites. The technique used to obtain these results is based on fluorescence microscopy. The work for the images is attributed to Dr. Mithila Burute from the lab of Prof. Kapitein at Utrecht University. Measurements in figure 2.1 were taken with 1 minute time interval. Time is increasing from left to right and up to bottom. The green color depicts the density of kinesins. The red color depicts the rest of the axon. The cell body is on the top left of the pictures. As one can see, the bulk of the kinesins is moving towards the cell body.

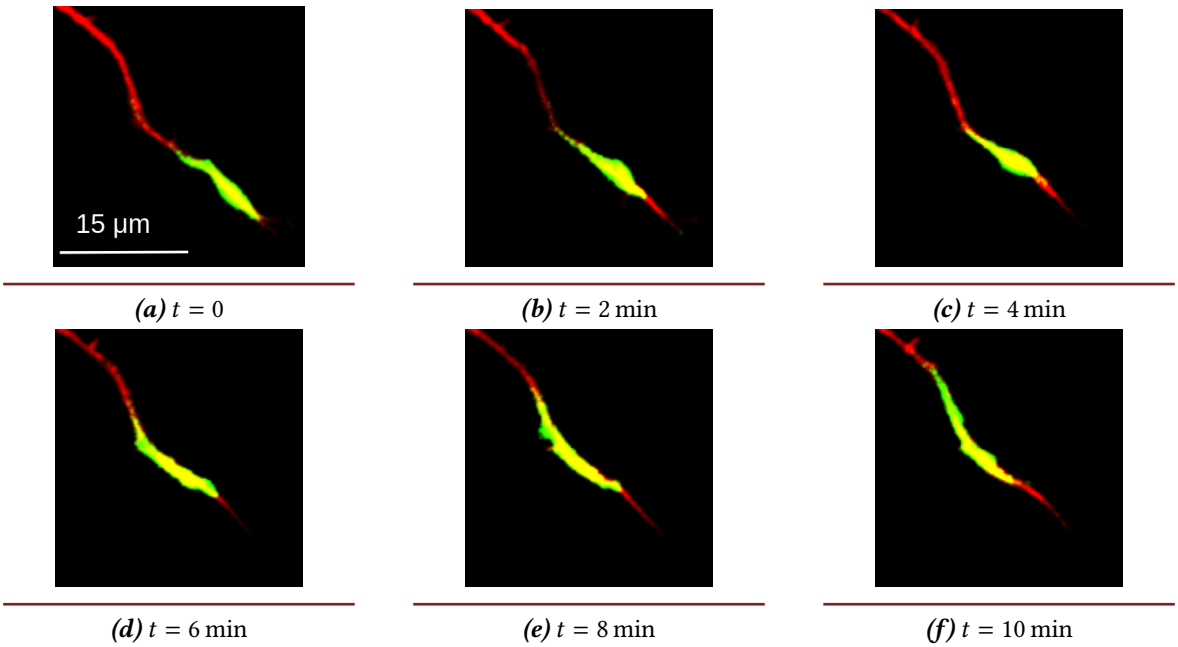

(a) $t = 0$ ***(b)*** $t = 2\,\text{min}$ ***(c)*** $t = 4\,\text{min}$

(d) $t = 6\,\text{min}$ ***(e)*** $t = 8\,\text{min}$ ***(f)*** $t = 10\,\text{min}$

Figure 2.1: *Images of moving kinesin (green and yellow) in a neurite (red). They depict the behavior of the kinesins for different times as noted in the sub-captions and reveal the motion to the cell body. The cell body, not in this image, is on the upper-left area of the images attributed to Dr Mithila Burute (unpublished data).*

We used ImageJ to process the images in figure 2.1 and extracted the density profile at different times. We define a line of a certain width (in pixels) over the axon and measure the intensity of the green color. The software averages automatically the intensity of pixels along the width of the line. In figure 2.2, we present the results of this analysis where the line width is 8 pixels. This approach has the following issue since the axon does not have a fixed radius. If we increase the width of the line then the software includes into the calculation void areas. On the other hand, if we decrease it, we neglect areas with kinesin molecules. It is hard to find the right balance. However, we can make some basic observations concerning the behavior of the kinesin desnsity, based on figure 2.2.

1. Since it is hard to extract a clear form of the density profile, we care for the main characteristics such as the bulk speed (speed of the whole profile, can be compared to the group velocity), the maximum of the profile, and the slope of the profile.
2. The density spreads out as a function of time.
3. We suspect that we cannot make a distinction between bound and unbound kinesin molecules. That is why we note the total density as $f(x,t)$.

4. The slope of the profile, which we define as the linear increment of the left siteof the profile, seems to be decreasing slowly. This is not a rigorous argument though, since it is hard to define a slope. We consider a line starting from the maximum and ending at the first zero points on its right.

5. Apart from the third line $t = 12$ min where the peak is at the same height as the peak of the second line $t = 6$ min, it seems that the maximum is decreasing. The cause is that the radius of the axon is smaller in that region and hence the concentration increases.

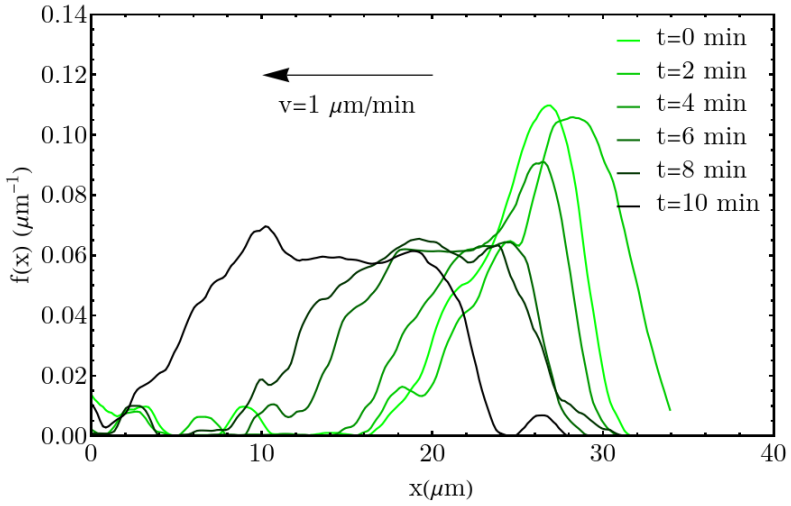

Figure 2.2: *The normalized density f(x) of bound an unbound kinesin molecules along the neurite for different time points. The position x = 0 corresponds to the edge of the image towards the cell body. The normalization is based on the density time* $t = 0$.

2.2 Geometry of the neurite

A typical neurite as the one shown in figure 2.1 has a length of 30 μm and a radius of 3 μm. For this reason, we can conceptualize it as a cylinder of that length and radius. We define a coordinate system where the zero is at the cell body and the positive direction of the x-axis is along the neurite pointing to the tip. Also, because the radius is small compared to the length we assume that the values of the physical quantities, such as the diffusion coefficient, are homogeneous vertically to the length of the cylinder. Hence their space dependence, if it exists, is only one dimensional.

2.3 Filaments

The elongated shape of neurites and later the axon is mostly determined by a network of cytoskeleton filaments. Actin and microtubule filaments are the two major networks that provide the structure to the cell. While actin forms a highly crosslinked network close to the cell membrane at the periphery, microtuble networks provide long filamental structures. Furthermore these long microtubule serve as highways for molecular motors that drive intracellular transport.

Microtubules are polymers of the subunits α- and β- tubulin (figure 2.3). These subunits connect and form a dimer. Then these dimers polymerize and create a microtubule. In humans, microtubules consist of 13 protofilaments which are linear rows of tubulin heterodimers. In that way from a distance, a microtubule seems to have a spiral shape. This gives the tubule a directionality; one end is indicated as '+END' and the other as '-END'. In neurites 80% of the microtubules have their +END toward the tip of the neurite [4].

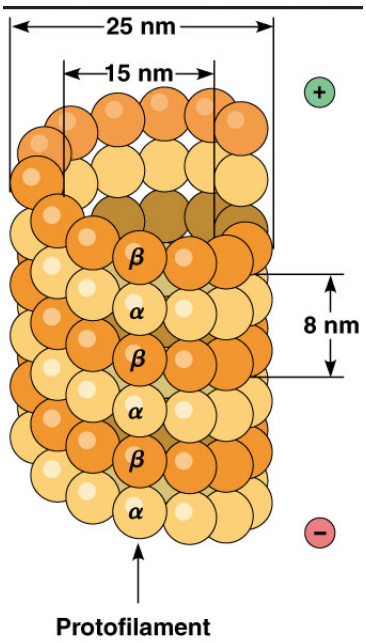

Figure 2.3: *The structure of a microtubule, reproduced from [2]. We see that heterodimers of α, β tubulins polymerize and form the microtubule. Its chiral shape allows us to define a directionality. For that reason we denote the ends of the microtubule as $+, -$. These ends are depicted by the circles with the corresponding signs.*

2.4 Molecular motors

Molecular motors are proteins that can bind to microtubules and perform an oriented walk by hydrolyzing ATP. Their molecular structure and function are different and determine the family they belong to. The most common families are called kinesin, dynein, and myosin. The experimental data we theoretically describe in this thesis concern the motion of kinesin-1, because the experiments used this type. For simplicity, we will use the group term kinesin to refer to kinesin-1 molecule. These molecules bind to microtubules and walk along them. Figure 2.4 shows the main structure of a kinesin. These molecules consist of two main (*"or heavy"*, colored in orange) chains and two lighter ones (colored in purple) [10]. The cargo binds in the area of the light chains. On the other side, the two sphere-shaped structures called heads, serve as attachment points to the microtubules. During the stepping process (see below) these heads bind to and unbind from microtubule filaments, respectively. For that reason, they can be functionally compared to the legs of a human.

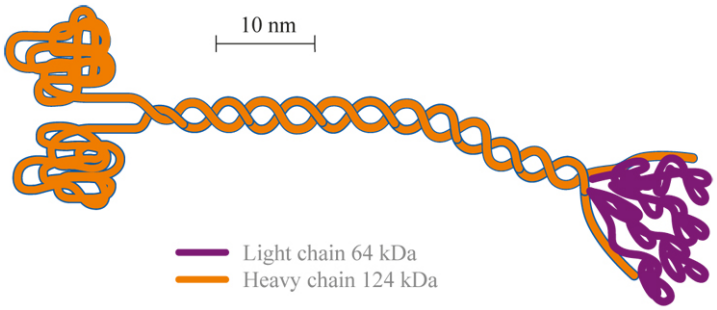

Figure 2.4: *Structure of kinesin, reproduced from [10]. The light chains colored in purple attach to the cargo, whereas the spherical structures at the end of the heavy chains (colored in orange) serve as attachment points to the microtubule. During the stepping process they perform a hand over hand motion that results in a phenomenologically walking movement.*

2.5 Stepping of kinesin molecules on the microtubules

When kinesins are bound to the microtubule they perform a stepping process that can be compared to that of a human. Tubulins act as sites where the heads of a motor protein can bind. During each stepping cycle, ATP binds to the front head and induces a strongly bound state with the microtubule. The front head (A) thus remains strongly attached to the microtubule. Simultaneously the second head (B) unbinds and rebinds to the site in front of head A. Then the products of the ATP hydrolysis ADP and a phosphate group are released

from the head B which is now in front and the cycle repeats (see figure 2.5). The way the second head moves forward is not certain. The most accepted way of this process is called 'hand over hand' [3, 9, 14].

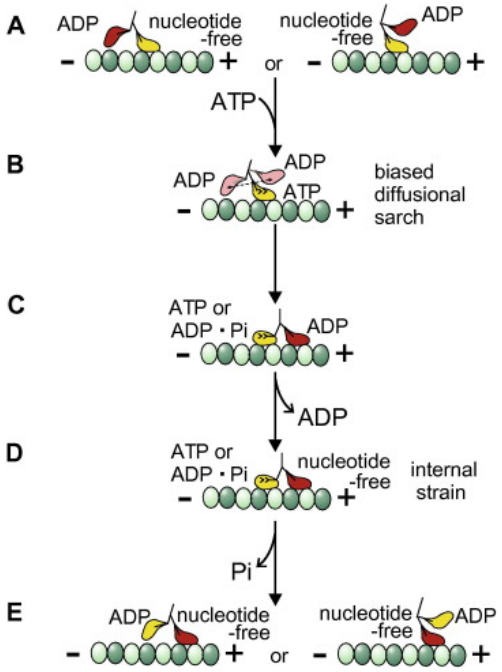

Figure 2.5: *Mechanism of stepping. A, E: Starting position. One head is attached to the microtubule, while a P group is released as a byproduct from the previous cycle. The ADP molecule remains attached. B: An ATP molecule is attached to the head in front. The other head is performing a hand-over-hand motion and attaches weakly to the microtubule in front of the first head. C, D: ATP is hydrolyzed and ADP from the second head is released. Reproduced from [3]*

In this thesis, we are mostly interested in the macroscopic behavior of a system of many kinesins. In this regime, the time-averaged motion of the density of kinesins $b = b(x,t)$ is described mathematically by the transport equation

$$\partial_t b + v\partial_x b = 0, \tag{2.1}$$

where we assume that the +END of the microtubule coincides with the positive direction of the x-axis (as it is the most probable scenario. see sections 2.2, 2.3) and v is the speed of a single kinesin molecule. As one can imagine v depends on the step rate of the kinesin. The step rate depends on many biological factors, but the most important is the ATP concentration because it provides the free energy that is needed for this process to happen [5].

When we include more kinesins we include an extra factor in the transport equations which now reads:

$$\partial_t b + v\partial_x b(1-b) = 0, \tag{2.2}$$

The reasoning for this additional factor is that a kinesin might block another kinesin to step forward. Mathematically this equation is named as *"Totally Asymmetric Simple Exclusion Principle" (TASEP)* and we study it in the rest of the section. There is a wealth of literature on TASEP but the features we are interested in are described in [8]. In the following, we summarize the most important points for our investigations:

- This form of equation (2.2) assumes that $0 < b(x,t) < 1$. However, in practice we want to normalise the density by requiring:

  $$\frac{1}{a}\int_0^L b(x,t)\mathrm{d}x = 1, \quad t > 0,$$

  where a is the normalisation factor. In that way, using the normalised density in equation 2.2, then it reads

  $$\partial_t b + v\partial_x \left[b(1-ab)\right] = 0, \tag{2.3}$$

  where we also made a coordinate transformation. For the rest of the thesis, we consider only normalized densities because the experimental evidence is given in that way and thus we use only equation 2.3.

- The local speed of the density is

  $$v' = 1 - 2ab. \tag{2.4}$$

  We can use this formula to calculate theoretically the speed of any point with density value b, but we are usually interested in the maximum of the density profile.

- When we have a finite system then the density shape takes a triangular form. This is shown in figure 2.6.

For validation, we solve equation 2.5 numerically and run a particle simulation of the system. Details about these approaches are given in the appendix.

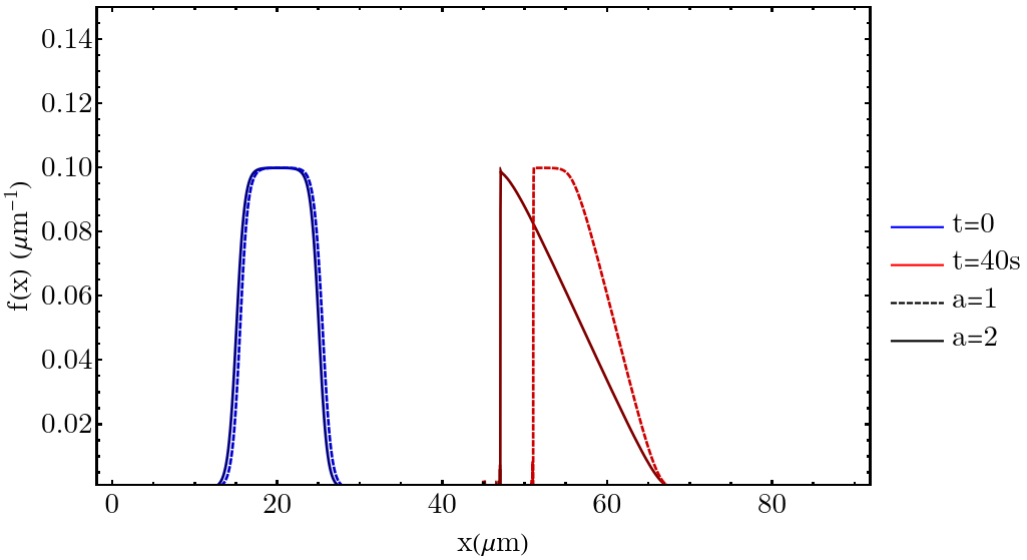

Figure 2.6: *Numerical solutions of the system 2.3 for two different values of a as noted in the legend. We see that the higher the parameter a the more drastic the deformation of the density. The shape becomes triangular more rapidly.*

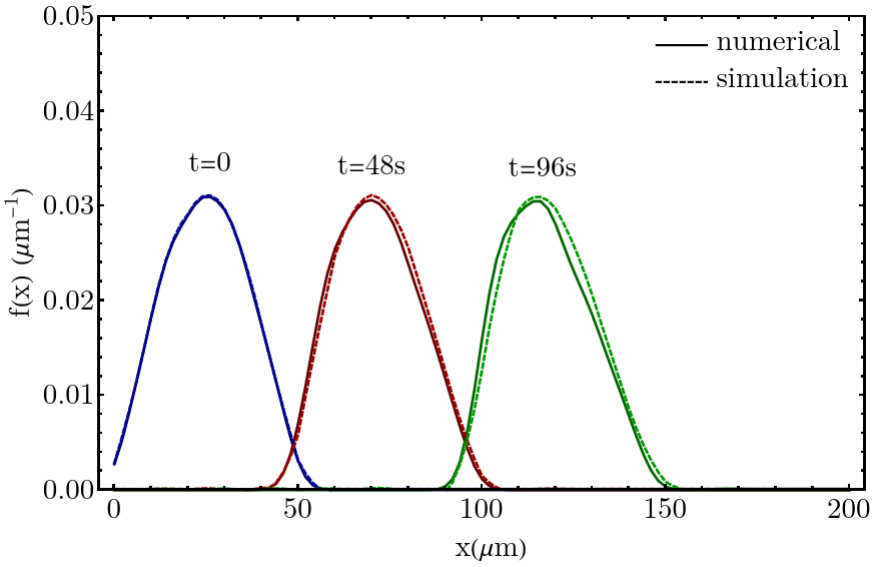

Figure 2.7: *Comparison of numerical analysis and simulation for the jamming effect (equation 2.3 with $a = 1$). Solid lines represent numerical results, whereas dotted ones are produced from a simulation. The difference in colors stands for different time points, which are written above each group of lines. The initial profile is a sinusoidal distribution. Units are arbitrary. In this case, because of the smoother profile, the numerical solution does not introduce errors and thus we can compare the two methods for a longer total time. We ran 10 simulations and we took the average. The standard error is very small (< 0.001).*

2.6 Diffusion of unbound kinesin molecules

When kinesin molecules are unbound from the microtubule filaments they perform a non-oriented Brownian motion. This motion occurs when a tracer particle is embedded in a liquid or gas. Such a particle is subjected to the small and random variations of the forces that act on them by the molecules of the dilute medium (e.g., water). On a macroscopic scale, this process is equivalent to that of a diffusion, where the diffusion coefficient is described by the Stokes-Einstein relation

$$D = \frac{k_B T}{6\pi\eta R}, \tag{2.5}$$

where η is the fluid viscosity and R the effective hydrodynamic radius of the particle, $k_B T$ is the thermal energy and π is the known mathematical constant [1].

The cytosol is comprised mostly of water and ions such as Sodium (Na^+), Potassium (Ka^+), and Calcium (Ca^{2+}). Hence, the viscosity of that medium is similar to that of pure water. However, fibers and structures that exist inside the cell act as a net, which hinders the motion of larger particles. Hence, the diffusion coefficient varies from that described by the Stokes-Einstein equation by a factor of $10 - 100$ for particles with a size larger than 100 nm.

Specifically for kinesin molecules as referenced in [12] we get

$$D = 1 - 2.5\ \mu m^2/s.$$

Finally, because the size of kinesins is small and the system we consider includes a large amount of them we consider the evolution of the density of these molecules (*a function of space and time*), rather than the motion of individual molecules. The time evolution of such a density obeys the diffusion equation:

$$\partial_t u = \partial_x \left(D \partial_x u \right), \tag{2.6}$$

where $u = u(x, t)$ is the density of unbound kinesin molecules and $D = D(x, t)$ the diffusion coefficient[1]. This specific form of heat (*diffusion*) equation implies that D is not constant, but it is spatio-temporal dependent.

[1] We pick this letter to symbolise the density because we denote the bound density as $b = b(x, t)$.

2.7 Interaction of kinesin molecules and microtubules

Kinesin molecules bind to microtubules. This binding process involves several steps that are not well understood. Kinesin molecules diffuse to the vicinity of microtubules, a process that could be influenced by electrostatic interactions. Once they are close to the microtubules they can form a bond with the microtubule. The size of the vicinity is of the order of the kinesin's size, approximately 100 from the microtubule. For simplicity, we can effectively describe this procedure as a stochastic process. When a motor is at time $t_0 = 0$ at a distance of less than 100 nm from the microtubule, then there is a probability that in the time interval $[0, \Delta t]$ it binds to it [12]. We can describe this via an exponential distribution $P(t)$ which obeys the following relation,

$$P(t) = \pi_0 e^{-\pi_0 t}, \tag{2.7}$$

where π_0 is the rate constant for binding, which characterizes the system. According to [11, 12] the rate parameter has a numerical value of $\pi_0 = 5\ \mathrm{s}^{-1}$. The notation is inspired by these studies. So far we examined the case where the kinesin molecule is in the vicinity of the microtubule. However, most of the unbound kinesin molecules are not. For that reason, we need to include an extra factor Φ that counts for the probability that a kinesin molecule is near the microtubule. This factor depends on the radius of the axon and the number of microtubules. For a typical case, this is of order $\Phi = 10^3 - 10^4$ which results in an effective binding rate of $\pi = 5\ 10^3\ \mathrm{s}^{-1}$ [12]. Similarly, the unbinding process is described stochastically. In this case, however, the physical mechanism can be traced down to the thermal motion of water molecules and consequently the collision with the kinesins that break the motor microtubule bonds. The rate parameter for the unbinding process is $\epsilon = 1\ \mathrm{s}^{-1}$ [12].

In terms of kinesin densities, we can describe these processes by two "reaction equations" which read:

$$\begin{aligned} \partial_t u &= \epsilon b - \pi u \\ \partial_t b &= -\epsilon b + \pi u, \end{aligned} \tag{2.8}$$

where u, b is the density of unbound and bound kinesins respectively.

In this form we have not included the hard-core exclusion as in section 2.5. If we do, the system reads:

$$\begin{aligned} \partial_t u &= \epsilon b(1-u) - \pi u(1-b) \\ \partial_t b &= -\epsilon b(1-u) + \pi u(1-b). \end{aligned} \tag{2.9}$$

For completeness of our description, we note that:

- We can include a similar factor as in the section 2.5 so that we can use the normalized densities in this description.
- However, we do not do that because we usually simplify the system in such a way that these hard-core exclusions are insignificant.

Finally as a validation we present a comparison between the numerical solution of the system 2.8 and the corresponding particle simulation (figure 2.8). We assumed an initial condition that is homogeneous along the x-axis. For that reason we omit that dependence in the plot.

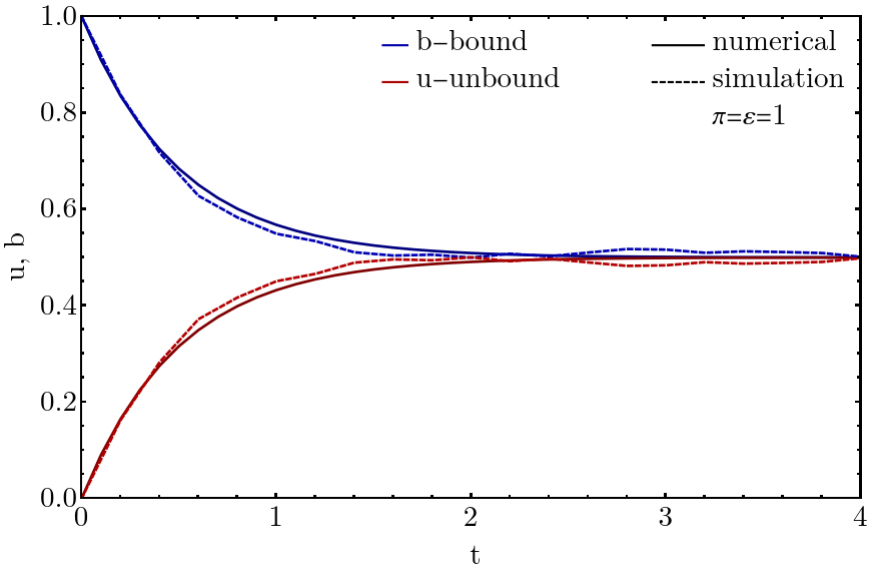

Figure 2.8: *Results for the system of ODEs equation 2.8. The upper lines depict the bound density whereas the lower the unbound. We also compare simulation (dashed) with numerical solution (solid). There is coherence between those two methods.*

2.8 Mathematical description of a typical system of kinesin movement

In this section, we combine the knowledge of the previous sections and present the mathematical description of a typical system of kinesins in a neurite. For the completeness of our description, we present different models based on a discretized and a continuous space. However, we mostly use the second one. As one can see in figure 2.9 if we discretize the space and create a 2D-lattice where the first row from the bottom represents the microtubule, then a kinesin acts differently when unbound from or bound to the microtubule. When unbound it diffuses in the cytosol or binds to the microtubule if it is near it with a rate π_0. When a kinesin is bound to the microtubule then it can unbind with rate ϵ or it tries to step forward. Unless the site is empty the step is rejected. As discussed in section 2.7 we can multiply π_0 with a factor that accounts for the probability that a kinesin is near the microtubule. In that way, we have an effective binding rate. With that being said we present a table of the values of these parameters. In the second column, we report the values found in the literature, while in the third column we present the values we use for our models unless we explicitly note otherwise [11, 12].

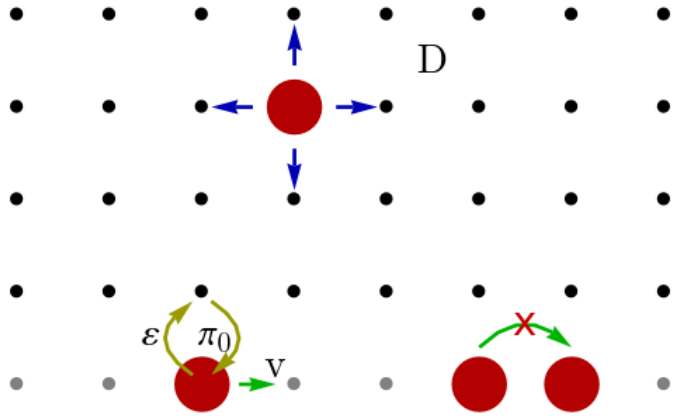

Figure 2.9: *A discrete model of the system. An unbound kinesin diffuses or binds to the microtubule (grey dots) if it is near to it. A bound kinesin steps forward or unbinds. If a kinesin tries to step forward but the site is not empty then the step is rejected (hard-core exclusion).*

symbol	values in literature	values used in this study
D	$0.5 - 2.5\mu m^2/s$	$1\mu m^2/s$
π_0	$5 - 10s^{-1}$	$5s^{-1}$
π	$10^3 - 10^4 s^{-1}$	$10^4 s^{-1}$
ϵ	$1s^{-1}$	$1s^{-1}$
v	$0.68 - 1.2\mu m/s$	$1\mu m/s$

Table 2.1: *The range of the numerical values for the parameters that are of our interest is given in the second column. In the third column, we present the specific numerical value that we chose for our simulations. We call these values "typical".*

Next, we present the continuum model. In this case, the density of kinesins is represented by two space-time-dependent functions. One for the bound kinesins $b = b(x,t)$ and one for the unbound $u = u(x,t)$. The mathematical system is one of two coupled partial differential equations (PDEs) which reads:

$$\begin{aligned} \partial_t u &= \overbrace{\partial_x \left(D\partial_x u\right)}^{\text{diffusion}} + \overbrace{\epsilon b(1-u) - \pi u(1-b)}^{\text{reaction term}} \\ \partial_t b &= \underbrace{-v\partial_x(b(1-ab))}_{\text{transport}} - \underbrace{\epsilon b(1-u) + \pi u(1-b)}_{\text{reaction term}}. \end{aligned} \tag{2.10}$$

The first equation describes the diffusion of the unbound density whereas the second equation describes the time evolution of the bound density. The physical meaning of each term is explained with an under-over brace. This system can be derived by the discrete model if we take the limit that the length of each siteand time step goes to zero. For more information on this derivation, one can look at [12].

One might also want to non-dimensionalize the system. We do this by considering the substitutions

$$\begin{aligned} t \longrightarrow t' &:= \pi t \\ x \longrightarrow x' &:= \frac{\epsilon}{v} x \end{aligned} \tag{2.11}$$

and defining the quantities

$$\begin{aligned} d &:= \frac{\epsilon}{v^2} D \\ k &:= \frac{\epsilon}{\pi}. \end{aligned} \tag{2.12}$$

The system then reads

$$\begin{aligned}\partial_t u =& \partial_x \left(kd\partial_x u\right) + kb(1-u) - u(1-b)\\ \partial_t b =& -\partial_x(b(1-b)) - kb(1-u) + u(1-b),\end{aligned} \tag{2.13}$$

where we have omitted the prime notation for simplicity.

We point out that we could make other substitutions to create non-dimensional quantities. This specific choice is more advantageous though because it makes clear that some terms can be neglected as typically $k = \frac{\pi}{\epsilon} \ll 1$, see table 2.1. Also, since $v = 1\ \frac{\mu\text{m}}{\text{s}}$, $\epsilon = 1\ \text{s}^{-1}$ the values of x remain the same although they have no dimensions. In addition if we try to find the local reactive equilibrium by requiring that the reaction terms equal to zero, i.e.,

$$kb(1-u) = u(1-b),$$

we find that

$$u \approx 10^{-3} b.$$

That means the majority of the kinesins are bound to the microtubule.

In the next chapters, we use this set of equations as a basis for the mathematical description of our models. A final note concerns the boundary conditions (b.c.) and initial conditions (i.c.). The experimental results are not very conclusive on the exact form of the behavior of the densities (see section 2.1). However, the density at the cell body is almost zero for the period we are interested in and we know that the tip of the neurite is a wall for the kinesins. They cannot get out of the cell. For that reasons we require:

$$b(0,t) = 0, \quad u(0,t) = 0,$$

$$\partial_x b|_{x=L} = 0, \quad \partial_x u|_{x=L} = 0.$$

As the initial condition we use either a normal distribution or the experimental profile at $t = 0$.

Chapter 3

Diffusion model

In this chapter, we examine the hypothesis that the diffusion coefficient is spatio-temporal dependent. Biophysically this idea is inspired by the observation that a cell can precisely regulate the polymerization of the actin meshwork that is a major constituent part of the cellular environment. A rapid change of the actin meshwork will change the diffusion behavior of molecules within this space. Such actin polymerization waves have been associated with the transport of molecular motors in neurites [6]. After the kinesin molecules have reached the end of the neurite, actin polymerization starts and pushes the kinesins back to the cell body by locally changing the effective diffusion coefficient. We introduce this effective diffusion coefficient to describe the fact that larger molecules such as kinesin motors are locale trapped and hence diffusion is hindered.

Consequently, in an environment where the diffusion coefficient is not constant, some particles, initially bound to the microtubule, unbind and diffuse faster in the direction towards the cell body. Then they rebind to the microtubule and the same process is repeated giving the impression of a backward movement.

The profile of the diffusion coefficient is not known, neither the exact mechanism that drives this process. However, we can disprove this hypothesis.

The first argument against this idea is inspired by the non-dimensionalized system 2.13. As one can see, diffusion is described by the term

$$\partial_x \left(kd\partial_x u \right).$$

Since, $d\ k \approx 10^{-3} \ll 1$, the diffusion term is negligible. Hence it cannot affect the system that drastically.

A second argument arises if we consider the Péclet number of the process which is defined

as

$$P = \frac{l_D\, v}{D},$$

where $l_D = vt$ is the characteristic length scale. Thus

$$P = \frac{v^2 t}{D}.$$

For diffusion to counteract the active transport of kinesin molecules it must be $P < 1$ or equivalently

$$D > v^2 t.$$

While for small time scales *(i.e., seconds)* diffusion might indeed overcome the active transport of kinesins, for longer periods active transport has always a more drastic effect.

Finally, for sanity, we solve numerically the main system (equation 2.13) and present the corresponding results (figure 3.1) for two different values of the diffusion coefficient as noted in figure. The reason we do this is to show that diffusion has an insignificant effect even when the coefficient increases drastically. We use a Gaussian distribution as the i.c.

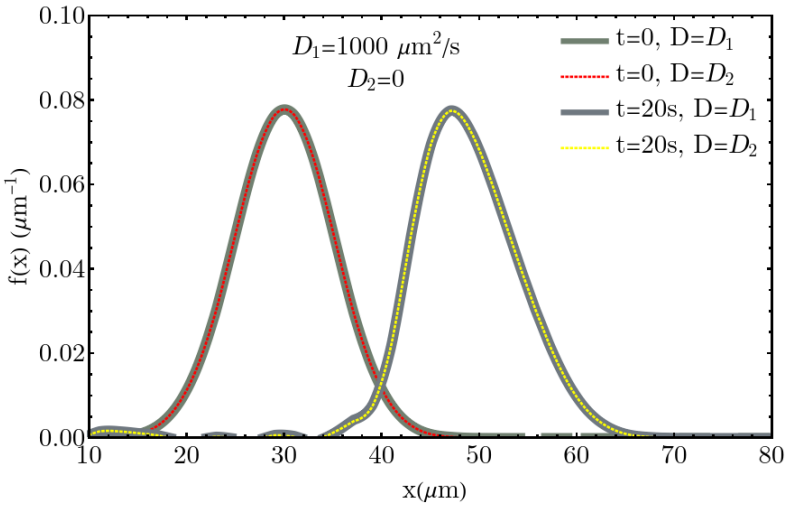

Figure 3.1: *The numerical solutions of the main system (equation 2.10), for two diffusion coefficients as noted in the plot. Even with that difference of the diffusion coefficient there is no difference in the behavior of the density of kinesins $f(x,t)$. The i.c. is a normal distribution and we use the b.c. we described in section 2.8.*

One can see that there is no difference between the results of the main system (equation 2.13), although there is a large difference of the diffusion coefficient. This plot confirms that diffusion is indeed ineffective in creating back transport.

Chapter 4

Binding-Affinity model

In this chapter, we examine a model based on the hypothesis that $\pi = \pi(x,t) \geq \tilde{\pi}$, where $\tilde{\pi}$ is the typical value as introduced in section 2.8. The case where $\pi < \tilde{\pi}$. The biophysical motivation behind this scenario follows from a similar concept as the diffusion model and we do not report in detail it here. Initially, all kinesins walk to the tip of the neurite. At the time t_0 the microtubules are modified in such a way that a region with a high affinity and a region with a low affinity for kinesin emerges. To examine this hypothesis we solve the main system (equation 2.13) numerically.

First, we need to define a specific form of the binding affinity $\pi(x,t)$. Because we do not have any biological insight on how this could look like we consider two different profiles. The first one is a step function, and the second is a sinusoidal function. Both have the same maximum value. The reason for this choice is that a monotonic function may affect the system differently than a periodic one, although the peaks and the troughs are the same in both cases.

As explained in section 2.8 we reach a reactive equilibrium when $u = 10^{-2}b$. That means the factor $(1-u) \approx 1$ and hence it can be neglected. Also, because $dk \approx 10^{-3}$, we can neglect the diffusion term. Finally we assume that $a = 1$. For the above reasons, we do not need to plot the unbound density, since it is almost zero. With these changes, the system reads:

$$\partial_t u = kb - u(1-b) \tag{4.1}$$

$$\partial_t b = -k\partial_x(b(1-b)) - kb + u(1-b), \tag{4.2}$$

After we find the numerical solution we reintroduce the dimensions.

I: Step profile for the binding affinity

For the form of the step-wise binding affinity depicted in figure 4.1 and described by

$$\pi(x,t) = 10^3 \left[1 + \frac{10}{1 + e^{-3(x+t-35)}}\right]^{-1},$$

we obtain the results shown in figure 4.2.

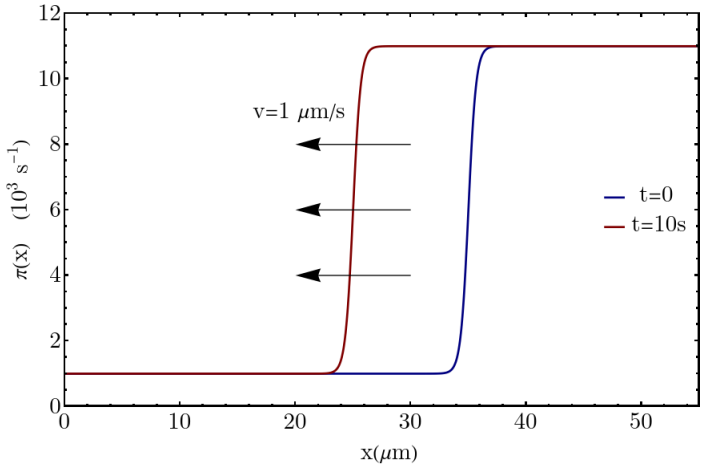

Figure 4.1: *The binding rate $\pi(x,t)$ as a function of space and time that we use for the numerical solution of the system 2.13. Since, the normal value of $\pi = 10^3$ s^{-1} (see section 2.8) we use a proper scaling so that one can see the relative difference between the normal value and the value we use for this case. The horizontal axis depicts the position along the neurite. We plot two lines for moments in time 10 seconds apart as written in the legend.*

As one can see in figure (4.2) the bulk of the density is moving forward to the tip of the neurite. The value of the maximum is approximately is 0.08 and it moves with an average speed of 0.85 $\frac{\mu m}{s}$ as one can estimate by reading the graph. We can calculate this speed also theoretically by using the formula for the TASEP (equation 2.4) as introduced in section 2.5. Since $a = 1$ we get

$$v' = (1 - 2b)v.$$

Hence after substitution of the numerical values we get $v' = 0.84$ $\frac{\mu m}{s}$ which coincides with the numerical results. This coherence suggests that the change of the binding rate in space and time has no significant effect on the system. Hence, we can disprove this profile.

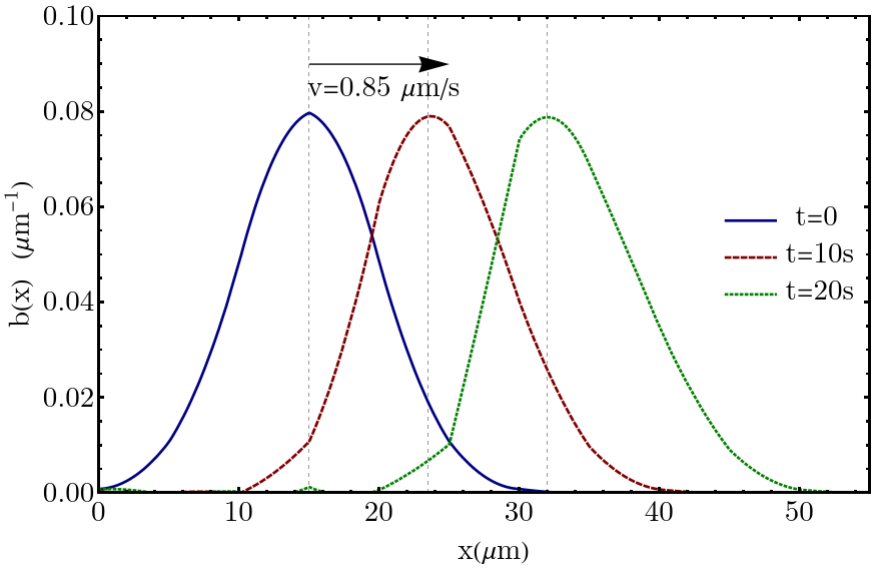

Figure 4.2: *The bound density $b(x,t)$ as a function of space. The horizontal axis depicts the position of the neurite (after reintroducing dimensions). The density is normalized so that the area equals to 1. We plot three lines for different moments in time as written on top of the lines. One can see that the change of binding affinity has an insignificant contribution to the evolution of the profile.*

II: Sinusoidal profile for the binding rate

In the second case, we use a profile for the binding rate of a sinusoidal function given by,

$$\pi(x,t) = 10^3 \left[1 + \left(\sin\left(\frac{x+t}{10}\right)\right)^2\right].$$

We depict this in figure 4.3. As one can see there is no difference compared to the case I (compare figure 4.2 and figure 4.4) and thus we are convinced that this hypothesis cannot explain the experimental evidence.

A final argument against this idea is that since $u \approx 10^{-2} b$ a further increase in the binding rate would not result in a significant difference because the "reservoir" of the unbound kinesins is already too small and almost all kinesins are already bound to the microtubule.

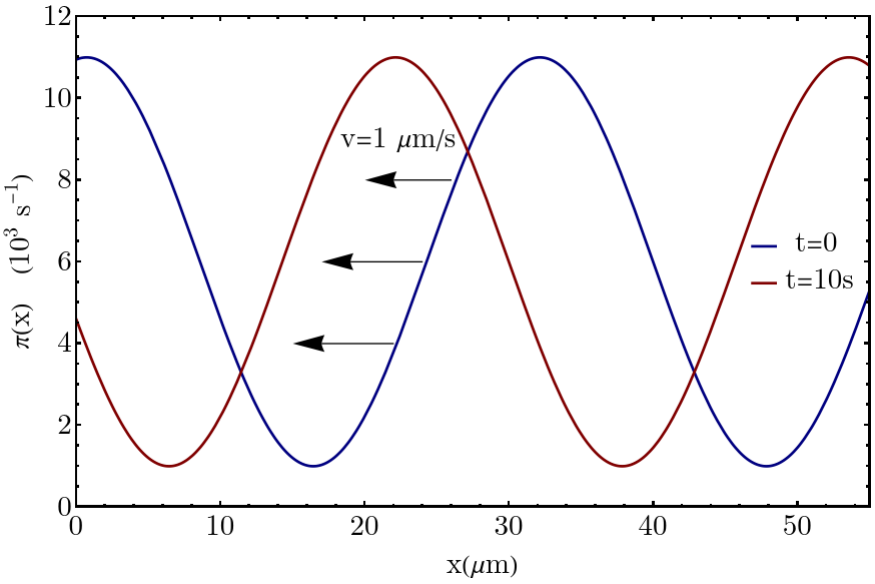

Figure 4.3: *The binding rate $\pi(x,t)$ used for the numerical simulation in subsection II. The horizontal axis depicts the position of the neurite. We plot three lines for different moments in time as written in the graph.*

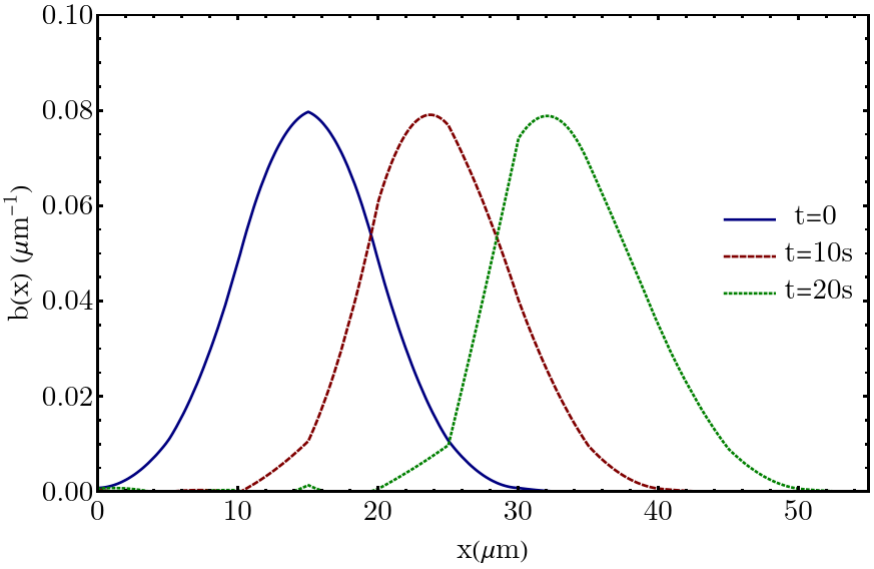

Figure 4.4: *The bound density $b(x,t)$ as a function of space. The horizontal axis depicts the position of the neurite, whereas the vertical the value of $b(x,t)$. The density is normalised. We plot three lines for different moments in time as written on top of the lines.*

4.1 Inclusion of microtubules oriented toward the cell body

As mentioned in section 2.3, neurites contain microtubules directed in both directions. The exact percentage of them having their +END to the tip of the neurite is not known firmly, but it is estimated that this number is close to 80% [4]. In this section, we take this property into account.

First, we define a third kinesin density $c = c(x, t)$, describing motors that are bound to the microtubules pointing to the cell body and thus move backwards. The temporal and spatial evolution of this density is described mathematically by an extra differential equation, similar to that of $b(x, t)$. The system in this case, before non-dimensionalization reads:

$$\begin{aligned}
\partial_t u =& d\partial_x^2 u + \epsilon(b + c)\ (1 - u) - \pi\ u(1 - r\ b - (1 - r)\ c) \\
\partial_t b =& -\partial_x(b(1 - b)) - \epsilon b\ (1 - u) + r\ \pi\ u(1 - b) \\
\partial_t c =& \partial_x(c(1 - c)) - \epsilon c\ (1 - u) + (1 - r)\ \pi\ u(1 - c),
\end{aligned} \tag{4.3}$$

where r is the percentage of the microtubules that have their +END at the tip of the neurite. From here on we set $r = 0.8$ as it is biologically the most accepted value.

We need to pay attention to the first equation, which describes the unbound density. In this system compared to those introduced previously, the behavior of the unbound density is affected by the sum of $c + b$. Also, there is no direct coupling between b and c, as they do not interact directly. Finally we note for completeness that the reaction terms cancel out. In that way, if we assume reflective b.c. in both ends then we also have conservation of motor proteins. Similar to the previous cases, we can non-dimesionalize the system and perform the same simplifications as in the previous section of this chapter. This results in:

$$\begin{aligned}
\partial_t u =& k(b + c) - u(1 - 0.8b - 0.2c) \\
\partial_t b =& -k\partial_x(b(1 - b)) - kb + 0.8u(1 - b) \\
\partial_t c =& k\partial_x(c(1 - c)) - kc + 0.2u(1 - c).
\end{aligned} \tag{4.4}$$

Below, we present the numerical solutions of these equations. The form of the parameter $\pi(x, t)$ is the step-wise function used in case (I) and is depicted in figure 4.1.

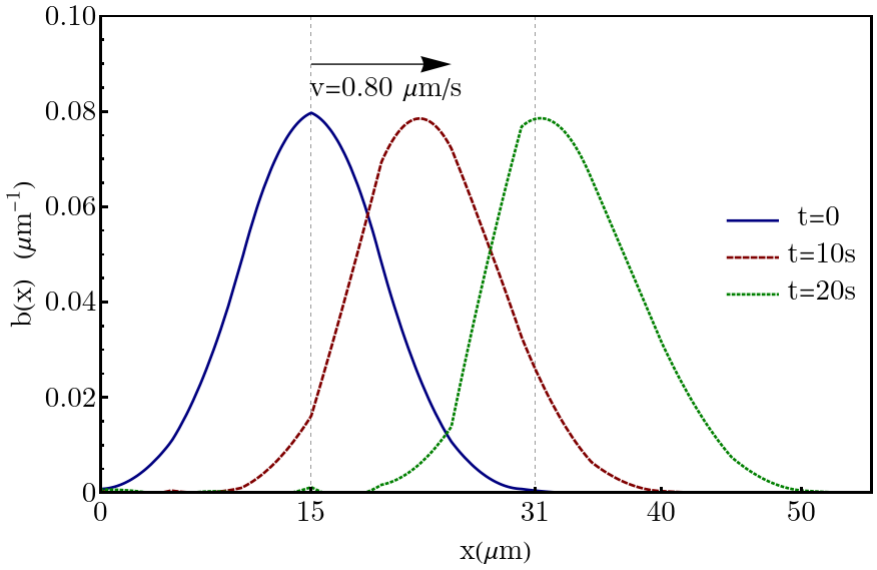

(a)

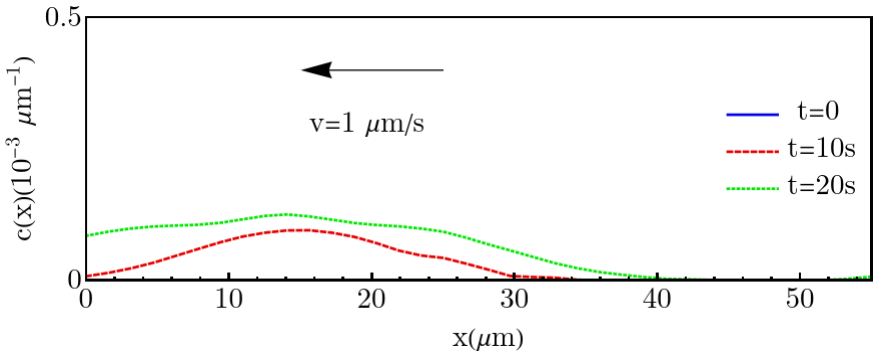

(b)

Figure 4.5: *a) Bound density profile of the kinesin motors that walk to the tip of the neurite. b)Bound density of the kinesin motors that walk to the cell body. Even in this case the final results show negligible difference with the previous cases. Initially all motors are bound to the "right" moving microtubules.*

One can see in figure 4.5 that even in this model there is little difference compared (compare figure 4.2 and figure 4.5) with the main model considered in this chapter. Still, most of the motors are bound to the microtubules. Also, because b interacts with c indirectly via the unbound density, the transition of kinesins between these two microtubules is very slow. As in the previous chapter, we can perform a speed analysis of the maximum point of b, by using the formula for the TASEP (equation 2.4). We find that $v_b = 1 - 2 \times 0.08 \approx 0.84\,\mu\text{m/s}$. Reading the graphs, one can confirm the value of v_b. The value for v_c is harder to confirm from the plots and thus we rely only on the theory. Because then $c(x,t) \ll 1$ we can

approximate the speed by setting $v_c = 1$ μm/s.

We can conclude that a space-time-dependent binding affinity cannot create the backward movement observed in the experiments, even if we include a subpopulation of microtubules that point towards the cell body.

Chapter 5

Two kinds of kinesins model

In this chapter, we examine the hypothesis that there are two kinds of kinesins which we note as kin-A and kin-B, and their densities are represented by the functions $b(x,t)$ and $c(x,t)$ respectively. Kin-A walks to the tip of the neurite whereas kin-B walks to the cell body. The biological reasoning for what might cause the appearance of these two different kinds is that either kinesin is directly or indirectly through an associated protein modified by some signaling cascade. This modification determines to which set of microtubules the motor binds to. To be more specific, kin-A binds to microtubules that have their +END at the tip of the neurite and hence they walk to the positive direction of the x-axis. For kin-B the opposite is true. In contrast to section 4.1 here, the binding to the minority of the microtubules, pointing to the cell body is deterministic.

In the beginning, there are only kin-A. At t_0 an unknown signaling cascade transforms all kin-A to kin-B. In that way, all kinesins bind to microtubules that point to the cell body. This results in the backward movement of the bulk. For this scenario, the corresponding system of equations can be divided into two time periods A and B.

In period A, kinesins cannot bind to microtubules pointing to the cell body Hence we only need the main system of equations (equation 2.13) which we simplify as we did in the previous chapter. Then it is written as:

$$\partial_t u = +kb(1-u) - u(1-b) \tag{5.1}$$

$$\partial_t b = -\partial_x(b(1-ab)) - kb(1-u) + u(1-b) \tag{5.2}$$

We note once more, that because $u \propto 10^{-3}b$ we can set the factor $(1-u) = 1$. We can also neglect the first equation describing the unbound density in total. To justify this drastic simplification we recall that $u = 10^{-2}b$, meaning that the majority of kinesins is bound to

the microtubules. In addition, we can consider the reaction term

$$kb - u(1-b).$$

Then since $k \ll 1$ the time needed for the reaction term to reach its equilibrium is too short compared to the time scales we are interested in. For that reason, we are allowed to assume that u is constant and that

$$b = \pi u(1-b), \tag{5.3}$$

meaning we have equilibrium in the reaction term. With these modifications, the system is simplified to a single equation which yields

$$\partial_t b = -\partial_x(b(1-b)). \tag{5.4}$$

During period B we have to add an equation for the left-moving kinesins and change some terms respectively in the other two. Let us show the system first and explain it later:

$$\begin{aligned} \partial_t u =& \partial_x\left(d\partial_x u\right) + (b+c)(1-u) - \pi u(1-c) \\ \partial_t b =& -\partial_x(b(1-b)) - b(1-u) \\ \partial_t c =& \partial_x(c(1-c)) - c(1-u) + \pi u(1-c) \end{aligned} \tag{5.5}$$

The first equation describes the dynamics of the unbound density as usual. Something that needs to be emphasized though is the last term. In contrast with what one might expect we do not have b terms since during period B, kinesins cannot directly bind to microtubules pointing to the tip of the neurite. This term is also missing from the next equation.

As before we can make the same simplifications, which result in

$$\partial_t b = -\partial_x(b(1-b)) - b \tag{5.6}$$

$$\partial_t c = \partial_x(c(1-c)) + b. \tag{5.7}$$

The only difference is that in this case, the reactive equilibrium is when the relation

$$(b+c)(1-u) - \pi u(1-c) = 0$$

holds. Hence, we used this relation for our simplification instead of $b - \pi u(1-b) = 0$. The numerical results of this system are shown in figure 5.1. We defined that $t_0 = \ 20$s. In the upper panel, we plot the behavior of kin-A. At t_0 it starts to decrease, while at the same time the density of kin-B increases. Then kin-B walks to the cell body. We see that the density is changing into a triangular shape. This shape change indicates that a jamming effect is prominent, as described by the TASEP, see section 2.5.

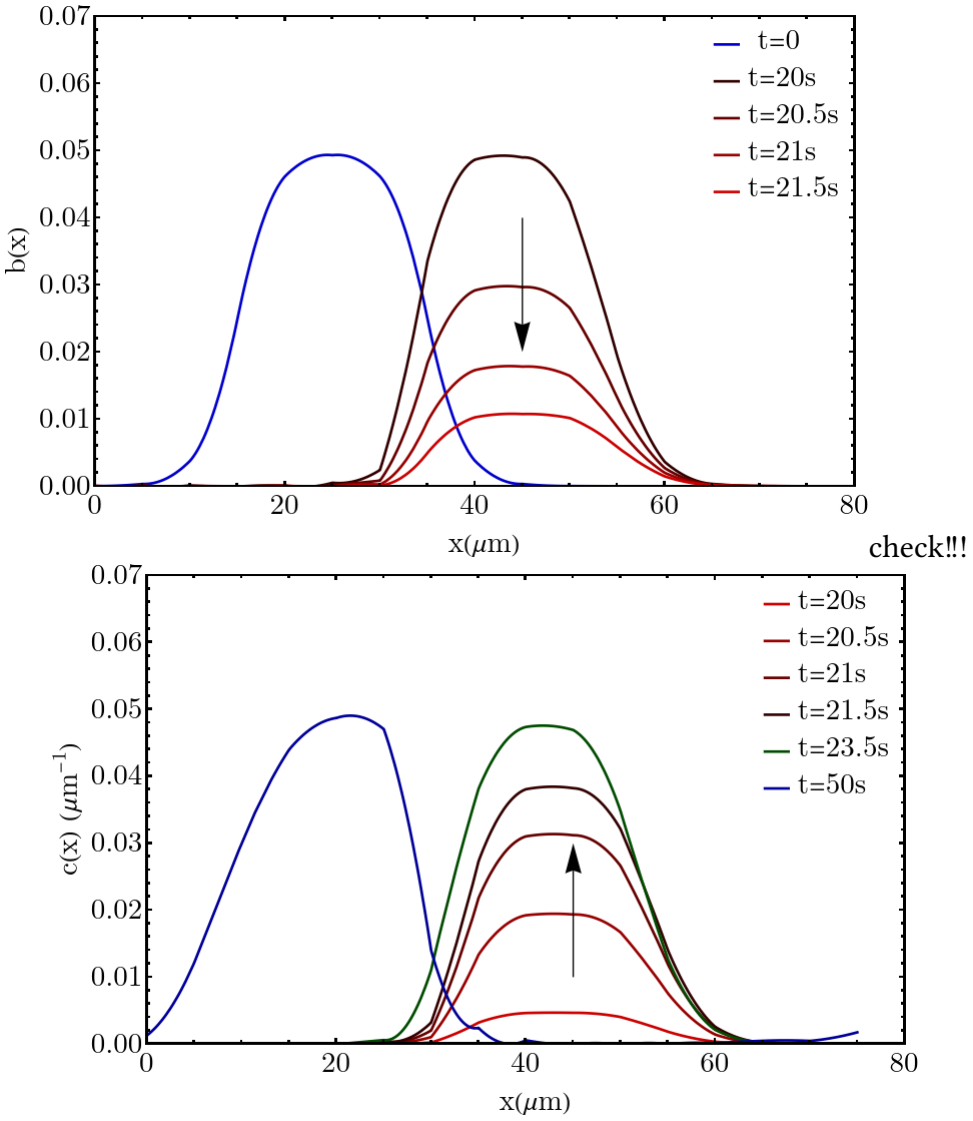

Figure 5.1: *The evolution of the density of kinesins. The upper plot depicts the right moving kinesins, whereas the lower depicts the left moving kinesins. Initially, the kinesins move to the right (described by b) and at time $t = 20$ s a cell-signaling cascade changes their binding affinity in such a way that they only bind to microtubules that point towards the cell body (to the left, described by c). At the lower graph, one can see the density increase and then move to the left (cell body). The velocity is not in line with the experimental evidence; it is too high.*

A problem we observe in this model concerns the average speed. As one can estimate by reading the figures the average speed $\langle v \rangle = 1\frac{\mu m}{s}$. However, the experimental results suggest that the average speed is $1\frac{\mu m}{min}$. We have tried to change the values of the physical constants

by one order of magnitude but the problem remains. Hence, something more subtle is happening.

To solve this problem we supplement the previous hypothesis with one biological phenomenon and introduce a physical concept. The biological phenomenon concerns a remodelling of the environment by induced actin polymerization. During this sub-process actin molecules polymerize inside the neurite with a speed of $\sim 2\ \frac{\mu m}{min}$! [6]. This is very similar to the speed of the bulk movement of kinesins as suggested by the experiments. Actin polymerization creates a very dense network in the cytosol, effectively reducing the binding rate of kinesin, as it hinders kinesins to approach the microtubules. At the same time, they block kinesins to diffuse in the cytosol. This results in a zero effective diffusion coefficient. The unbinding rate remains as before i.e., $\epsilon = 1\ s^{-1}$. In the following we investigate this idea systematically.

5.1 Speed reduction of the bulk by manipulation of the reaction terms

In this section we examine the following system:

$$\begin{aligned} \partial_t u &= \epsilon b - \pi u \\ \partial_t b &= -\partial_x \left[b(1-ab) \right] - \epsilon b + \pi u, \end{aligned} \tag{5.8}$$

where the notation is the same as in the main system (equation 2.13). Note that there is no reason to use an effective binding rate, because kinesins remain in the vicinity of the microtubule, thus for this system $\pi = \pi_0$.

We are interested in the sum $f = u + b$ because experimentally one cannot distinguish between bound and unbound particles when they are located at the same distance from the microscope (see section 2.1). Since particles, in this model, remain near to the microtubule they are at the same distance from the microscope as the bound ones, and thus they contribute to the kinesin profile of the experimental results. Our goal is to approximate the behavior of f by a simpler ODE. For that reason, we give a more intuitive approach to what is going on by considering the discrete system in figure 5.2 and specifically a cycle of binding and unbinding (figure 5.3).

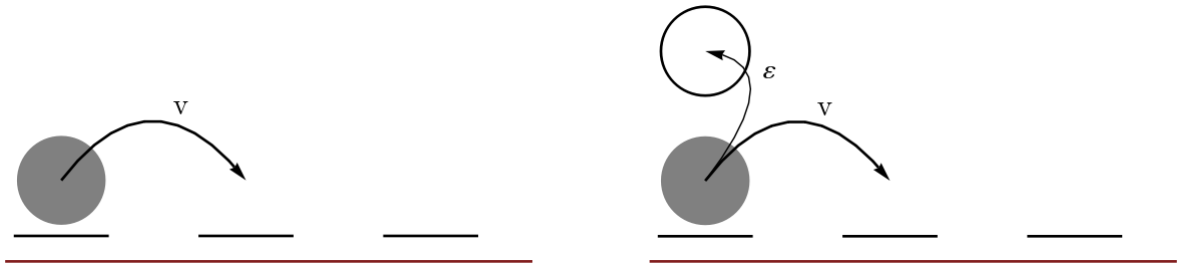

(a) *No reaction term* ***(b)*** *With reaction term*

Figure 5.2: *A schematic revealing the reason why a reaction term can cause a reduction in the observable speed of the density. When there is no reaction term (a) then the kinesin would step forward at each time step. In the other case (b) where we include the reaction terms, there is a probability that a kinesin will unbind and stop moving.*

In this system, we consider only one particle. When there are no reaction terms, then at each time step we expect that this particle moves one site. However, when we include reaction terms then there is a probability that this particle will unbind and stop moving until it rebinds. Hence, we expect that an outer observer will see that a particle will step fewer sites during the same number of cycles if reaction terms are present. Hence we can calculate the average distance covered in one cycle and therefore find its average speed. When we include more particles in the system, then we have to consider jamming effects described by the TASEP, as explained in section 2.5. In addition, because some particles remain unbound for a longer time the distance covered during a cycle differs. This means apart from the average distance we want to compute the mean squared of it and define a diffusion coefficient. As a conclusion, inspired by this physical motivation, we want to show that this system (equation 5.8) can be approximated by a single biased diffusion PDE. We refer to this concept as effective speed-reduction because the speed of the density we observe is lower than the speed of the walking kinesins.

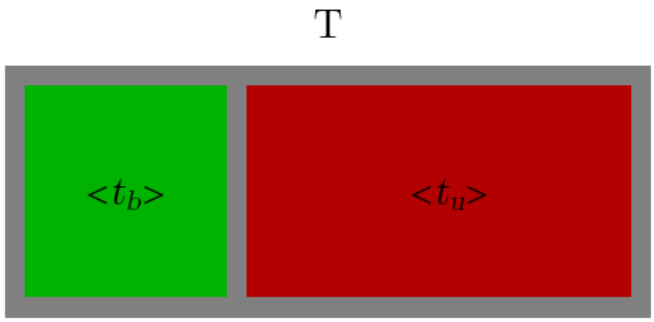

Figure 5.3: *A schematic of the work cycle of a period T. First a kinesin binds to the microtubule and remains bound (green) for an average of time $\langle t_b \rangle$ then it unbinds and remains unbound (red) for time $\langle t_u \rangle$. The cycle ends when the kinesin rebinds.*

First, we consider the system without any jamming effect (neglect hard-core exclusion) and we are limited to one cycle period, which we denote as T. During this period the particle remains bound for time t_b and unbound for time t_u (figure 5.3). Because both times are stochastic we can compute the mean values of them by considering their corresponding probabilities. As explained in section 2.7 these obey the exponential distribution,

$$P_b(t) = \epsilon e^{-\epsilon t}$$

$$P_u(t) = \pi e^{-\pi t}$$

Consequently, the average values are:

$$\langle t_b \rangle = \frac{1}{\epsilon}, \quad \langle t_u \rangle = \frac{1}{\pi},$$

In a similar fashion, we can also consider the probability that the particles either binds or unbinds to the microtubule. This probability, is given by the expression

$$P_{u||b}(t) = (\epsilon + \pi) e^{-(\epsilon+\pi)t}$$

Next we calculate the average time period and the average displacement of the particle $\langle (x - x_0) \rangle$. For simplicity we set $x_0 = 0$ and thus:

$$\begin{aligned} \langle T \rangle &= \langle t_b \rangle + \langle t_u \rangle \\ &= \frac{\pi + \epsilon}{\pi \epsilon}, \end{aligned} \tag{5.9}$$

$$\begin{aligned}\langle x\rangle &= \langle v t_b\rangle \\ &= v\langle t_b\rangle \\ &= v\frac{1}{\epsilon}.\end{aligned} \tag{5.10}$$

This equation is the average displacement during a cycle of average duration $\langle T\rangle$, which means the average speed is

$$\begin{aligned}v_{\text{eff.}} &= \frac{\langle x\rangle}{\langle T\rangle} \\ &= \frac{\pi}{\epsilon+\pi}v.\end{aligned} \tag{5.11}$$

Next, we want calculate the mean square of the displacement during a cycle. Since, both binding and unbinding are stochastic events and both affect the displacement of the particle we have to use the mean square of the probability distribution that contains information for both events. This distribution is the $P_{u||b}(t)$ with a mean square of

$$\frac{2}{(\epsilon+\pi)^2}.$$

Then, we can write that the mean square displacement over a cycle is given by:

$$\begin{aligned}\langle x^2\rangle &= v^2\langle t_{b||u}\rangle \\ &= v^2\frac{2}{(\pi+\epsilon)^2}.\end{aligned} \tag{5.12}$$

From that relation we can extract a diffusion coefficient by considering that $\langle x^2\rangle = 2dt = 2d\langle T\rangle$, which results in

$$d = v^2\frac{\pi\epsilon}{(\pi+\epsilon)^3} \tag{5.13}$$

Another way to arrive at the same result is by first writing the original system by Fourier transforming the densities. That allows us to write

$$\begin{aligned}\partial_t u &= \epsilon b - \pi u \\ \partial_t b &= -ikb - \epsilon b + \pi u,\end{aligned} \tag{5.14}$$

where k is the wavenumber and the densities are function of k i.e. $u = u(k,t),\ b = b(k,t)$. In addition, we supply this system with the initial conditions $b(k,0) = \frac{1}{\sqrt{2\pi}},\ u(k,0) = 0$.

The physical motivation behind this choice is that we want to derive the Green's function and thus in the phase space the total density is constrained on a single point which we can pick to be the origin of the x axis.

The system of equations 5.14 can be solved analytically. However, we are interested in the sum $f = u + b$, which obeys a very long relation. We present it for completeness of our description.

$$
\begin{aligned}
f(k,t) = & \frac{1}{\sqrt{2\pi}\sqrt{-(\epsilon+\pi)(\epsilon(i+k)^2)+(-i+k)^2\pi)}} \\
& \exp\left(-\frac{t\left(ik\epsilon+\sqrt{(-\epsilon-\pi)\left((k+i)^2\epsilon+\pi(k-i)^2\right)}-i\pi k+\epsilon+\pi\right)}{2(\epsilon+\pi)}\right) \\
& \left(\epsilon\left(-1+\exp\left(\frac{t\sqrt{(-\epsilon-\pi)\left((k+i)^2\epsilon+\pi(k-i)^2\right)}}{\epsilon+\pi}\right)\right)+\right. \\
& +\left(\pi+\sqrt{(-\epsilon-\pi)\left((k+i)^2\epsilon+\pi(k-i)^2\right)}\right)\exp\left(\frac{t\sqrt{(-\epsilon-\pi)\left((k+i)^2\epsilon+\pi(k-i)^2\right)}}{\epsilon+\pi}\right)+ \\
& \left.+\sqrt{(-\epsilon-\pi)\left((k+i)^2\epsilon+\pi(k-i)^2\right)}-\pi\right).
\end{aligned}
\tag{5.15}
$$

We can massage this expression (equation 5.15) by keeping only zero order of k in the polynomial terms and only second order of k in the exponential terms. This manipulation implies that the approximation works only for density profiles that their Fourier decomposition is limited on small values of wavelengths. In this thesis the profiles we test fit this condition and thus the approximation is valid. Proceeding with the simplification we can write

$$
f(k,t) = \frac{1}{\sqrt{2\pi}}\exp\left\{i\frac{\pi(\pi+\epsilon)+\pi-\epsilon}{(\epsilon+\pi)^2}vkt\right\}\exp\left\{-\frac{\pi\epsilon}{(\pi+\epsilon)^3}v^2k^2t\right\} \tag{5.16}
$$

Equation 5.16 is the Green's function of a biased-diffusion equation, suggesting in agreement with the previous method that the behavior of f can be described by a biased-diffusion equation, where the speed term takes the value of

$$
\frac{\pi(\pi+\epsilon)+\pi-\epsilon}{(\epsilon+\pi)^2}v
$$

and similarly the diffusion coefficient is

$$
\frac{\pi\epsilon}{(\pi+\epsilon)^3}v^2.
$$

Although it seems that these two methods do not agree on the value of the speed we note that

$$\frac{\pi(\pi+\epsilon)+\pi-\epsilon}{(\epsilon+\pi)^2} = \overbrace{\frac{\pi}{\pi+\epsilon}}^{A} + \overbrace{\frac{\pi-\epsilon}{(\pi+\epsilon)^2}}^{B}.$$

The term A is the same as that we found with the first method whereas the term B has an insignificant contribution to the overall speed for most of the values of $\pi,\ \epsilon$.

Summa summarum, we propose that the behavior of $f = u + b$, where u, b obey the system 5.8 can be approximated by the ODE:

$$\partial_t f = -v_{\text{eff.}}\partial_x + d\partial_x^2 f, \tag{5.17}$$

where the constants have been defined above (equation 5.13,5.11).

To test this suggestion we present a comparison between numerical solutions of the original system (neglecting hard-core exclusion) and the approximate system for non-dimensional constants (figure 5.5). We use a Gaussian density as i.c. and pick $\pi = 1$ and various values of ϵ as noted in the plots. There is excellent coherence between these two mathematical systems.

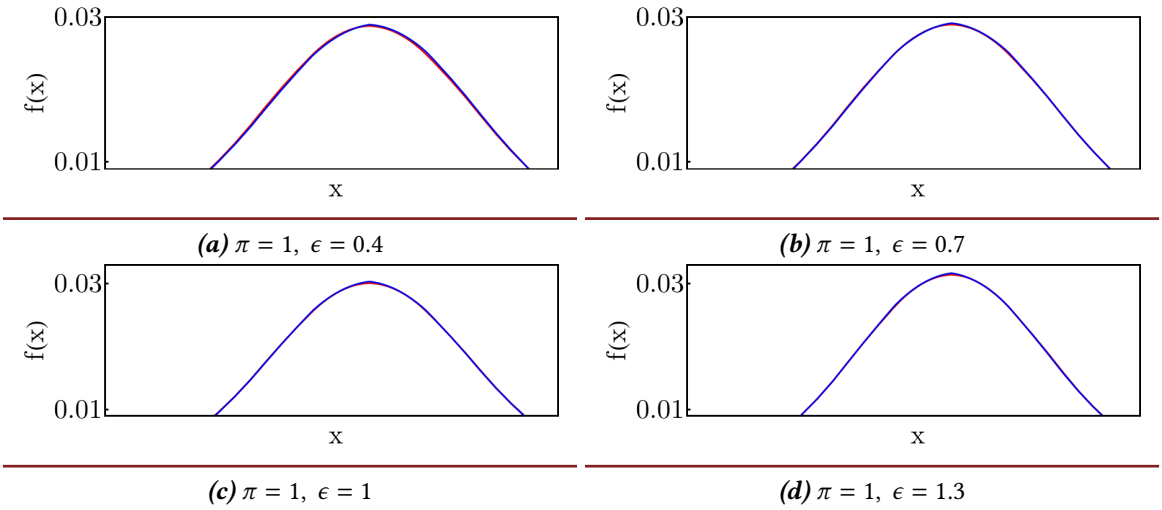

(a) $\pi = 1,\ \epsilon = 0.4$ ***(b)*** $\pi = 1,\ \epsilon = 0.7$

(c) $\pi = 1,\ \epsilon = 1$ ***(d)*** $\pi = 1,\ \epsilon = 1.3$

Figure 5.4: *The numerical solutions of the approximated and the original system (equation 5.1 neglecting hard-core exclusion, 5.17) for various values of ϵ at time $t = 800$. The blue line depicts the solution of the approximate equation whereas the red one represents the solution of the original system for the specific values that are mentioned under each subplot. The i.c. is a Gaussian profile. There is excellent coherence. For this simulation we used non dimensional units, while $v = 1$.*

Next we present two comparisons (figure 5.5) between the numerical solution of the approximate system (equation 5.17) and a particle simulation. We choose different values of π and ϵ as noted in the caption.

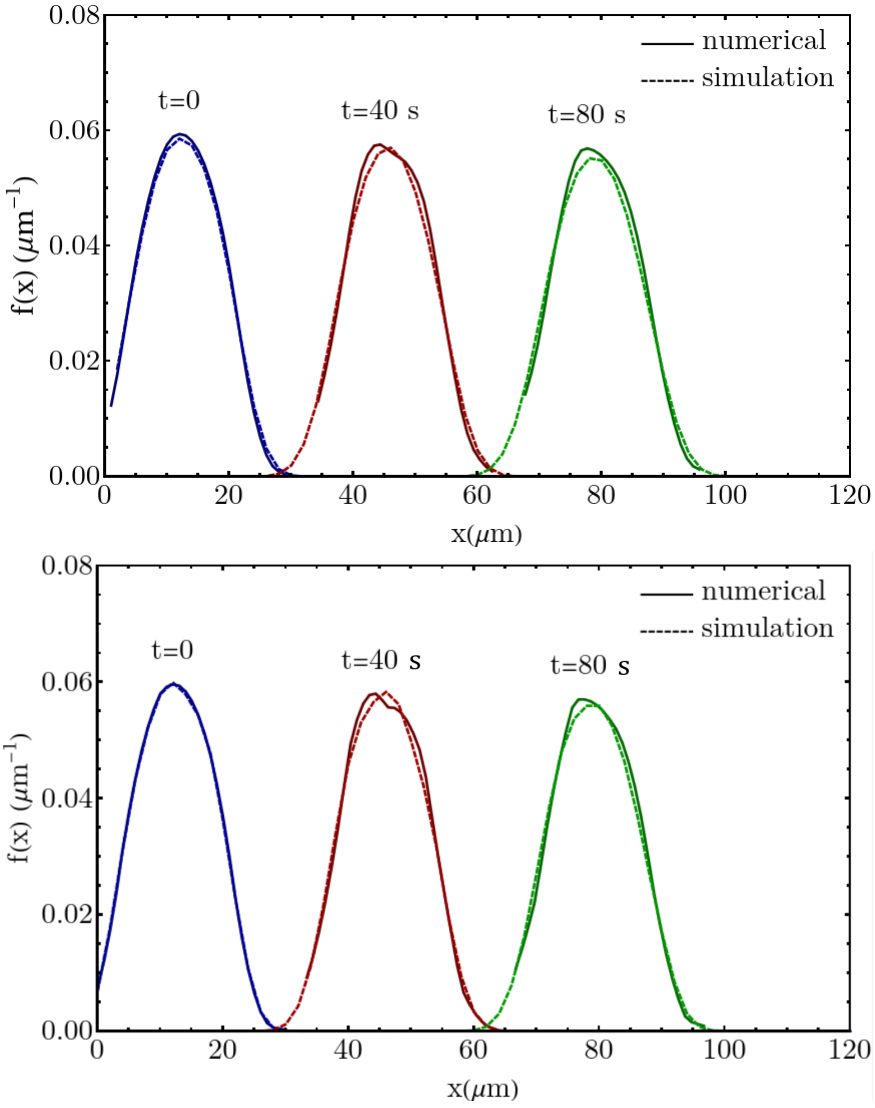

Figure 5.5: *Comparison of numerical and simulation results for the speed reduction effect (equation 5.8). Solid lines represent numerical results, whereas dotted ones are produced from a simulation. The difference in colors stands for different time points, which are written above each group of lines. The initial profile is generated randomly by the simulation and tries to approximate a normal distribution. It is the same as in figure 2.7. Here* $\epsilon = 0.1, 1\ \text{s}^{-1}$, $\pi = 0.5, 5\ \text{s}^{-1}$. *We run 10 simulations and we took the average. The standard error is very small* (< 0.001).

We point out that we have neglected hard-core exclusion in the reactive terms because as we noted at the beginning (see section 2.8) this effect is small. However, it is not unnoticeable and we show it later on.

At this point, we want to examine the system (equation 5.8) when we do not neglect the hard-core exclusion. To start our analysis we consider the discrete model. In contrast with the previous case, particles interact only and only if they are bound, which motivates us to calculate the average density of particles that are bound. This can be done either by considering the probability of one particle to be bound or by requiring that we are at reactive equilibrium. The result of either method is that the fraction

$$\frac{\pi}{\pi + \epsilon}$$

of all particles is bound.

Since we are speaking statistically and we have a large number of particles we can assume that the effect of the hard-core exclusion in this described system is the same as in the case of a system where the bound and unbound densities are ab initio

$$b = \frac{\pi}{\pi + \epsilon} f,$$

$$u = \frac{\epsilon}{\pi + \epsilon} f$$

respectively but without any further reaction terms. We justify that statement by first considering the following cases of the discrete model:

- A particle A is in front of another particle B and thus B cannot step. However, because A unbinds then the B is free to step, and thus the hard-core exclusion effect does not take place.
- A particle B has free sides to step but another particle A binds in front of it and blocks it from stepping forward. In this second case hard-core exclusion takes place despite the initial formation of the particles.

We suggest that these two processes, which are the only direct result of the reaction terms, cancel each other because the number of particles is large. For that reason, we can assume that the average number of particles that do not move because another particle is in front of them remains constant throughout the process. This simplifications allows to define an ODE by taking into account equation 5.17, which results in:

$$\partial_t f = -v_{\text{eff.}} \partial_x \left[f \left(1 - a \frac{\pi}{\pi + \epsilon} \right) f \right] + d \partial_x^2 f, \tag{5.18}$$

where $v_{\text{eff.}}$ and d are the same as before (equation 5.13, 5.11). Again, to test this suggestion, we present a comparison between numerical solutions of the original (equation 5.8) and the approximate system (equation 5.18).

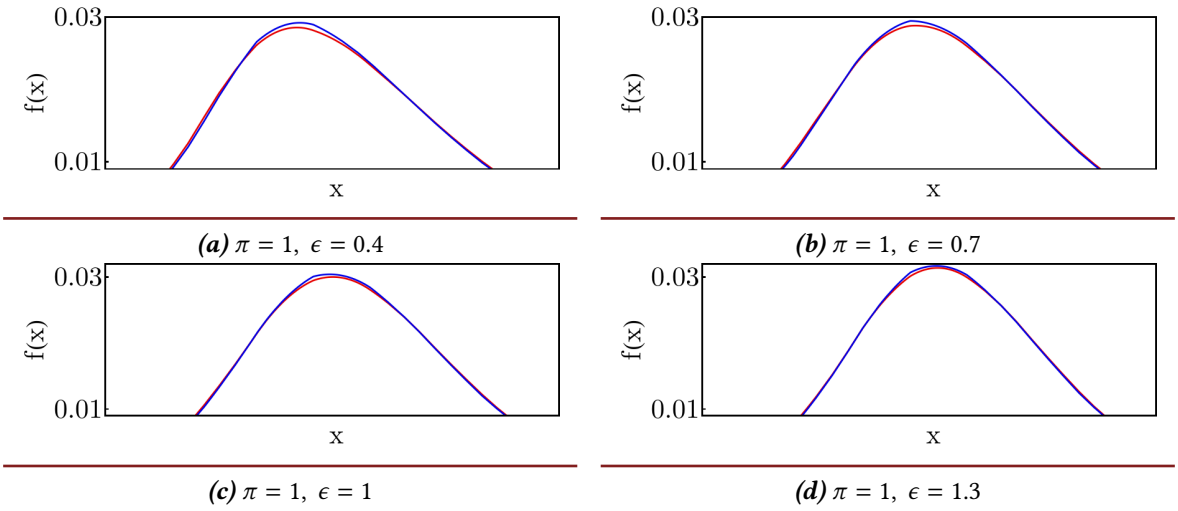

(a) $\pi = 1,\ \epsilon = 0.4$ ***(b)*** $\pi = 1,\ \epsilon = 0.7$

(c) $\pi = 1,\ \epsilon = 1$ ***(d)*** $\pi = 1,\ \epsilon = 1.3$

Figure 5.6: *The numerical solutions of the approximated and the original system (equation 5.1, 5.18) for various values of* ϵ *at time* $t = 800$*. The blue line depicts the solution of the approximate equation whereas the red one represents the solution of the original system for the specific values that are mentioned under each subplot. The i.c. is a Gaussian profile. There is great agreement. For this simulation we used non dimensional units and* $v = 1$*.*

One can see (figure 5.6) that there is a great agreement between the original and the approximate system when we solve them numerically. Finally, we present a graph where we compare the numerical results of the original system (equation 5.8), the numerical results of the approximate system (equation 5.18), and the particle simulation, see figure 5.7.

There is very good agreement among these methods which implies that we can use this approximation to describe our system. However, we cannotice the difference between simulation and numerical methods. This discrepancy is because we neglected hard-core exclusion in the reactive terms in the numerical results but not in the simulation. Finally, we note that equation (5.18) gives an intuition on this process and introduces the idea that the reaction terms effectively reduce the observable speed, which can be the reason why the speed in the experimental results is 60 times slower than the speed of the kinesin stepping.

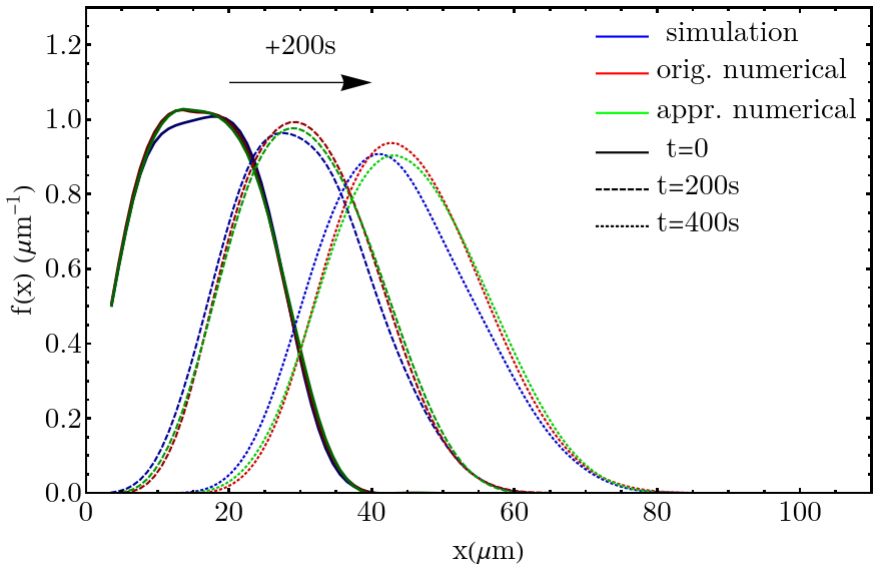

Figure 5.7: *Comparison of numerical and simulation results for a system described by (equation 5.8). Blue lines represent the simulation whereas red and green the numerical solution of the original and the approximated system (equation 5.18) respectively . Here* $\epsilon = 1.2\ \mathrm{s}^{-1}$, $\pi = 0.1\ \mathrm{s}^{-1}$. *We run 10 simulations and we took the average. The standard error is very small* (< 0.001).

5.2 Theoretical description of the experimental data

After the introduction of the approximation, we are now at a position to describe the experimental observation. We use equation 5.18 where we point out that since kinesins move to the negative direction of the x-axis we change the sign of the effective speed. We could set as i.c. the density of the experimental data at time $t = 0$ and fit the numerical solution to the experimental data. However, we cannot do that directly because as we can see in figure 2.2 at the beginning the density has a triangular shape and then it becomes rectangular. This behavior cannot be created by the approximated equation. We assume that this sudden deformation of the density arises either because of some external pressure at $t = 5$ min, that "squeezes" the neurite and hence the whole density flattens out, or because of actin contraction. For us this means, we can use this idea of a "quick spreading out" of the kinesins and implement it into our numerical solution by requiring that at time $t = 5$ min the density spreads out, because of a very short artificial diffusion term. Then after manually adjusting the physical constants, we find a solution using the values noted in table 5.1.

a	1
π	0.025 s^{-1}
ϵ	1 s^{-1}
v	0.7 μm/s

Table 5.1: *The values of the system 5.18 that gives rise to a solution that is close to the experimental results.*

Below, we present the numerical solution, where we used as i.c. the density profile of the experimental data at time $t = 0$. We need to point out that we had to smooth it by considering the moving average of 5 points. The reason for this is that, otherwise the numerical error is a million times larger than the density itself. In addition because it is almost impossible to reconstruct the accurate experimental profile (including fluctuations) in a particle simulation, we could only use a smoothed profile. However, we have already shown that numerical results are in agreement with simulations (section 5.1). Hence, using two methods would be redundancy, because neither method would be exact, since the i.c. is an approximation in either case.

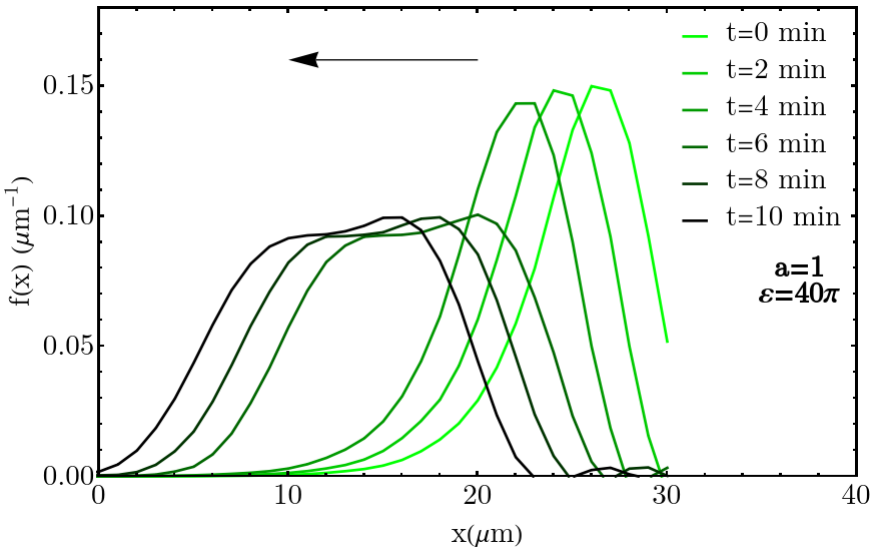

(a)

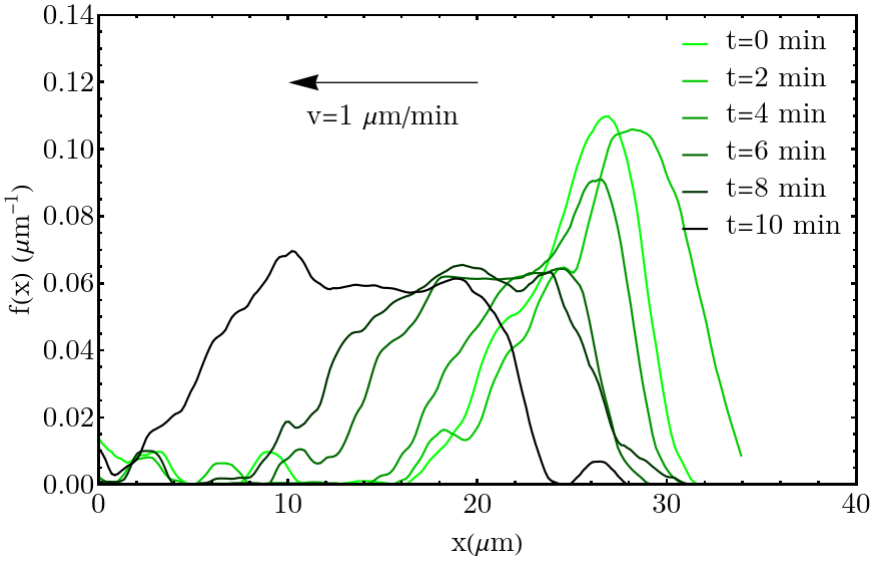

(b)

Figure 5.8: *a) The evolution of the density f as dictated by equation 5.18 using the values presented in 5.1. We also assume that at $t = 4$ min there is a spread of the kinesins along the neurite so that the length of the width in this plot is the same as in the experimental data. b) For easier comparison we present the experimental data at the lower panel.*

We see that some characteristics of the profile such as the average speed, the slope of both ends of the profiles, and the shape are very close to the experimental data. However, the maximum and the local speed are not. We cannot confirm this hypothesis, since more ex-

periments are needed, but it is a very accurate description of such systems that is introduced for first time in the field.

Chapter 6

Conclusion

In this thesis we discussed the main mechanisms that dictate the behavior of kinesins in a neurite (cylindrical geometry) and established the corresponding mathematical description of the system. Then, we presented experimental results that show a bulk movement of kinesins to the cell body, contrary to our knowledge of the mechanisms that dictate the behavior of kinesins. We examined perspective, three hypotheses that try to explain the reason of this unexpected behavior. The first two build on the idea that either the diffusion coefficient or the binding rate is spatio-temporal functions and not constants. The third hypothesis requires an explicit preference of kinesins to bind only to microtubules that result in a movement to the cell body. At the same time, an actin wave remodels the environment in such a way that the kinesins are not able to diffuse. This reduction of the diffusion also decreases the chance of the molecules to bind to microtubules. We rejected the first two hypothesis. For the third, we introduced an approximate description of the system and made more intuitive the behavior of the density at macroscopic level. However, we suggest the following experiments to obtain a better insight and test our theory. These are:

- Modification of the ATP concentration: It will effectively reduce the intrinsic step rate of the kinesins and consequently the value of the intrinsic speed we used. Hence, the average bulk velocity will decrease.
- Modification of the number of kinesins: It will increases the effect of the hard-core exclusion, and thus we expect that the slope of the density profile will increase at a lower rate.
- Modification of temperature: It will increase or decrease the value of the unbinding rate and thus we will observe a lower-higher bulk velocity and a lower slope rate.

ACKNOWLEDGMENTS

I would like to thank my supervisors Florian Berger and Joost de Graaf for sculpting the marble of my physical knowledge. Without their guidance, I would not be able to see the world of physics differently! I would also like to thank all of my teachers and professors that contribute to my education throughout the years. I hope this thesis counts as a reward for their efforts. Finally, I want to inscribe this thesis to my grandmother, my sister and to all of my friends for their unintentional support, when I need it the most.

APPENDIX

Numerical analysis

For the numerical solutions, we used the software Mathematica (version 12). Unless specified, it uses the Runge-Kutta method. The main disadvantage and obstacle are that the numerical error is large when the initial profile has steep regions, i.e, the derivative of the profile has a large value.

Particle simulation

Monte Carlo is a simulation method that uses pseudo-random number generators. Among different applications, this technique can be used to simulate many-particle systems and describe the properties of the steady-state. However, we never reach that state, and hence we name this method as particle simulation, although the main idea is the same. As explained in sections 3, 2.7, Brownian motion, and the binding and the unbinding process are stochastic processes. We implement this property by generating pseudo-numbers R in the range of $(0, 1)$. For each simulation, we define a 2D discretized lattice with X and Y sides and consider the first row as the microtubule. Also, we define a length of site l, a time step τ, and the number of kinesins N. Next we set

$$k_\epsilon = \epsilon\tau$$

and

$$k_\pi = \pi\tau.$$

These values are the probabilities that a kinesin will (un)bind during a time step. Finally, we declare an extra number b as the probability that a kinesin will move one site when bound during a time step[1]. These values are not independent and should obey the following

[1]We have included this number and feature to give an extra degree of freedom to the simulation

relations:

$$D = \frac{l^2}{4\tau} \tag{6.1}$$

$$v = \frac{l}{b\tau} \tag{6.2}$$

where D the diffusion coefficient and v the intrinsic speed of the kinesins.

A kinesin can be bound or unbound to the microtubule (first row). When unbound and also on the first row a random number dictates if it binds or diffuses. If $R < k_\pi$ then the kinesin binds otherwise it diffuses. When a kinesin is unbound but not on the first row then it diffuses. Finally, when a kinesin is bound to the microtubule a random number dictates if it unbinds. As before, if $R < k_\epsilon$ then it unbinds, otherwise a second random number is generated and dictates if it will step to the next side.

When we want to include hard-core exclusion we require that the step will be on an empty side, otherwise, it is rejected.

Bibliography

1. Einstein, A. Über die von der molekularkinetischen Theorie der Wärme geforderte Bewegung von in ruhenden Flüssigkeiten suspendierten Teilchen. *Annalen der Physik* **320,** 549–560 (1905).
2. Weisenberg, R. Microtubule Formation in vitro in Solutions Containing Low Calcium Concentrations. *Science* **177,** 1104–1105 (1972).
3. Kawaguchi, K. Energetics of kinesin-1 stepping mechanism. *FEBS Letters* **582,** 3719–3722 (2008).
4. Stone MC Roegiers F, R. M. Microtubules have opposite orientation in axons and dendrites of Drosophila neurons. *Molecular Biology Cell.* **19,** 4122–4129 (2008).
5. Clancy Bason, e. a. A universal pathway for kinesin stepping. *Nature structural molecular biology* **18,** 1020–1027 (2011).
6. Amy W Winas Sean R Collins, T. M. Waves of actin and microtubule polymerization drive microtubule-based transport and neurite growth before single axon formation. *eLife* **5** (2016).
7. Takano, T., Funahashi, Y. & Kaibuchi, K. Neuronal Polarity: Positive and Negative Feedback Signals. *Frontiers in Cell and Developmental Biology* **7,** 69 (2019).
8. Ferrari, P. A. TASEP hydrodynamics using microscopic characteristics. *Probability Surveys* **15,** 1–27.
9. Hancock, W. O. The Kinesin-1 Chemomechanical Cycle: Stepping Toward a Consensus. *Biophysical Journal* **110,** 1216–1225.
10. Hirokawa, N. *et al.* Submolecular domains of bovine brain kinesin identified by electron microscopy and monoclonal antibody decoration. *Cell* **56,** 867–878.
11. Lipowsky, R., Klumpp, S. & Nieuwenhuizen, T. M. Random walks of cytoskeletal motors in open and closed compartments. *Physical Review Letters* **87,** 1081–1101.
12. Müller, M. J., Klumpp, S. & Lipowsky, R. Bidirectional Transport by Molecular Motors: Enhanced Processivity and Response to External Forces. *Biophysical Journal* **98,** 2610–2618.

13. Ohashi, K. G. *et al.* Load-dependent detachment kinetics plays a key role in bidirectional cargo transport by kinesin and dynein. *Traffic* **20,** 284–294.

14. Yildiz, A. & Selvin, P. R. Kinesin: walking, crawling or sliding along? *Trends in Cell Biology* **15,** 112–120.

Ω